Figure S1

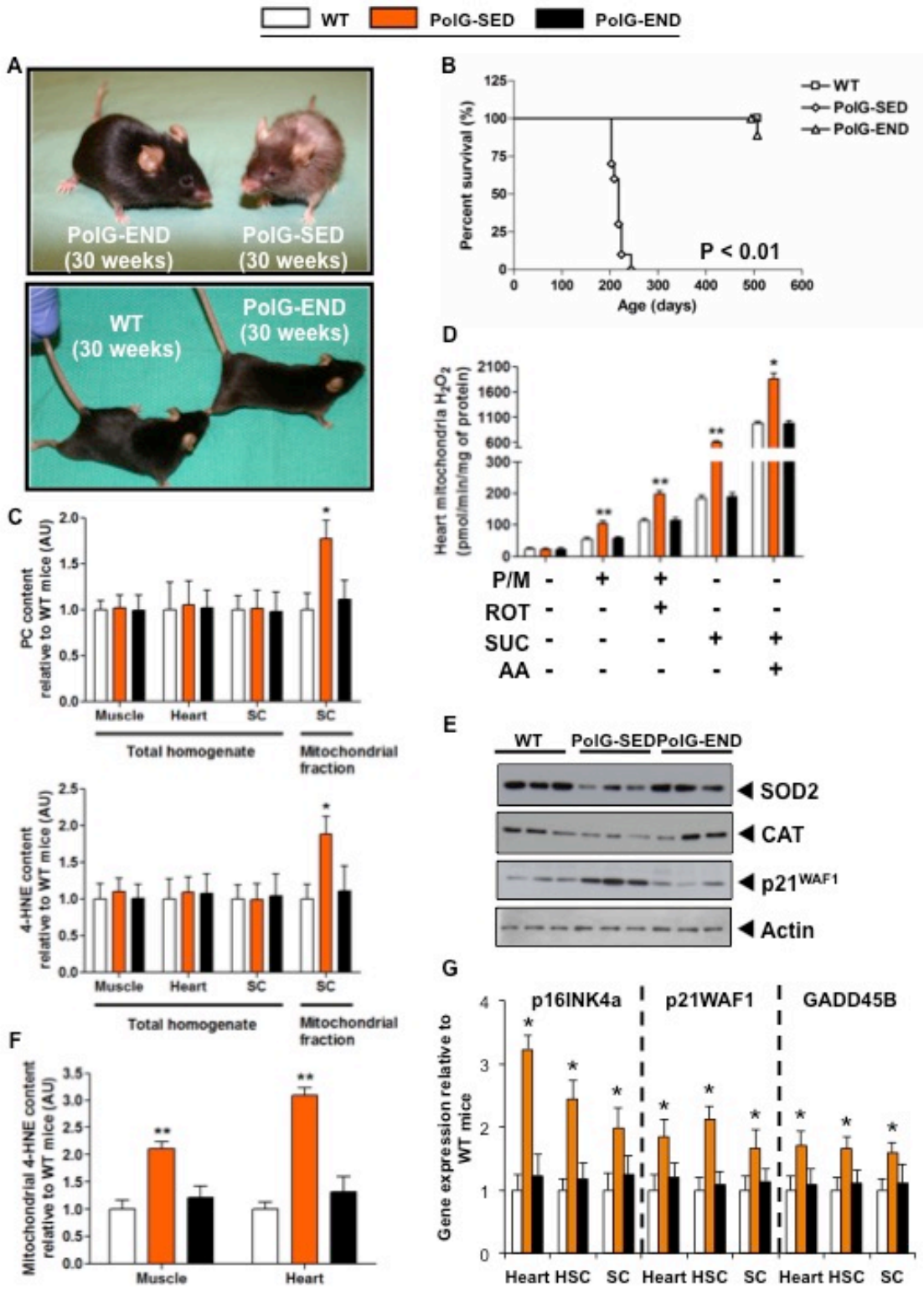
WT
PolG-SED
PolG-END
A
PolG-END (30 weeks)
PolG-SED (30 weeks)
WT (30 weeks)
PolG-END (30 weeks)
B
Percent survival (%)
Age (days)
P < 0.01
WT
PolG-SED
PolG-END
C
PC content relative to WT mice (AU)
Muscle
Heart
SC
SC
Total homogenate
Mitochondrial fraction
4-HNE content relative to WT mice (AU)
D
Heart mitochondria H_2O_2 (pmol/min/mg of protein)
P/M
ROT
SUC
AA
E
WT
PolG-SED
PolG-END
SOD2
CAT
p21WAF1
Actin
F
Mitochondrial 4-HNE content relative to WT mice (AU)
Muscle
Heart
G
Gene expression relative to WT mice
p16INK4a
p21WAF1
GADD45B
Heart
HSC
SC

Figure S1. Endurance exercise confers complete phenotype protection, suppresses early mortality, mitigates mitochondrial ROS-mediated oxidative damage, increases cellular antioxidant capacity, and prevents cellular senescencmutator mice. (**A**) Representative images from each group (~7.5 months of age) are displayed. The PolG mice in sedentary group (PolG-SED) showed progressive reduction in body size, increased kyphosis, loss of hair pigmentation and alopecia in comparison with littermate wild-type (WT) mice. Endurance exercise dramatically reversed the visible features of premature aging in PolG mice (PolG-END). (**B**) Endurance exercise suppresses early mortality reported in mtDNA mutator mice. Survival curves are significantly different ($P < 0.01$) between PolG-SED (◊, diamond) vs. WT (□, square) and PolG-END (Δ, triangle) mice (*n* = 5/group). The logrank test was used to test for significant differences in life span distribution between groups. (**C**) Protein carbonyls (PC; marker of protein oxidation) and 4-hydroxynonenal (4-HNE; marker of lipid peroxidation) content in muscle, heart, and SC total homogenate and satellite cell (SC) mitochondrial fraction of WT, PolG-SED, and PolG-END (n = 6-8/group). (**D**) H_2O_2 production rate in heart mitochondrial fractions of WT, PolG-SED, and PolG-END (n = 7-10/group). Complex I and II substrates: P/M, pyruvate/malate and SUC, succinate (5mM each), respectively. Complex I and III inhibitors: ROT, rotenone and antimycin A, AA (0.5 μM each), respectively. (**E**) Antioxidants mitochondrial superoxide dismutase 2 (SOD2; ~25 kDa) and catalase (~60 kDa) protein content, and marker of cellular senescence, p21WAF1 (~21 kDa) protein content (representative Western blot of muscle) in

muscle of WT, PolG-SED, and PolG-END (n = 4-6/group). Actin (~45 kDa) is used as a loading control. (**F**) 4-HNE content in muscle and heart mitochondrial fractions of WT, PolG-SED, and PolG-END (n = 4-6/group). (**G**) Expression of p53-mediated senescence markers: $p21^{WAF1}$, $p16^{INK4A}$, and GADD45B in heart, SC, and hematopoietic stem and progenitor cells (HSC) of WT, PolG-SED, and PolG-END (n = 4-6/group). Asterisk (PolG-SED vs. both WT and PolG-END): * $P < 0.05$, ** $P < 0.01$. Error bars represent SEM. AU, *arbitrary units*.

Figure S2

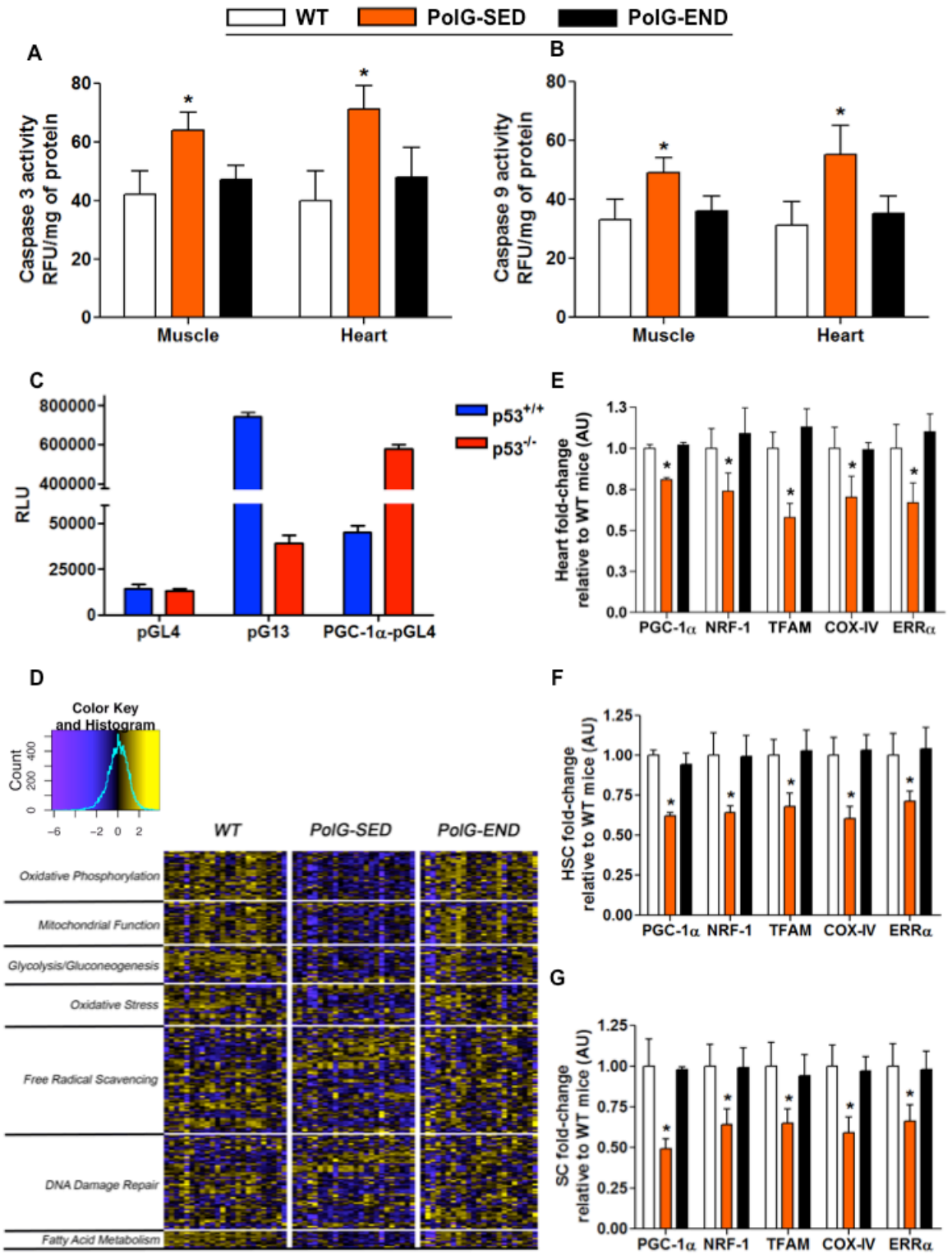
WT
PolG-SED
PolG-END
A
Caspase 3 activity RFU/mg of protein
Muscle
Heart
B
Caspase 9 activity RFU/mg of protein
C
RLU
p53+/+
p53-/-
pGL4
pG13
PGC-1α-pGL4
D
Color Key and Histogram
Count
WT
PolG-SED
PolG-END
Oxidative Phosphorylation
Mitochondrial Function
Glycolysis/Gluconeogenesis
Oxidative Stress
Free Radical Scavencing
DNA Damage Repair
Fatty Acid Metabolism
E
Heart fold-change relative to WT mice (AU)
PGC-1α
NRF-1
TFAM
COX-IV
ERRα
F
HSC fold-change relative to WT mice (AU)
G
SC fold-change relative to WT mice (AU)

Figure S2. Endurance exercise prevents dysregulated mitochondrial-induced apoptosis and reduces nuclear p53-mediated repression of PGC-1α and promotes mitochondrial biogenesis in mutator mice. Mitochondrial-induced apoptosis mediator (**A**) caspase 3 and (**B**) caspase 9 activity in muscle and heart of WT, PolG-SED, and PolG-END (n = 4-6/group). (**C**) p53 represses PGC-1α promoter reporter. MEFs from *p53*$^{+/+}$ and *p53*$^{-/-}$ mice were transfected with empty pGL4 luciferase reporter vector or pGL4 luciferase reporter vector with -2.8 kb fragment of mouse PGC-1α promoter encloned (three independent experiments). pG13 luciferase reporter plasmid (containing 13 copies of a synthetic p53 DNA binding site) was used as a positive control. RLU, *relative light units*. (**D**) Microarray-based Ingenuity Pathway Analysis of skeletal muscle shows enrichment of gene ontology categories of transcripts which are significantly over-represented in transcriptome (Fisher's exact test, n = 24/group). The gene probes within these categories are plotted as a heat map displaying the normalized expression changes within each gene. Expression pattern indicates that the changes between WT vs. PolG-SED are largely normalized through exercise in PolG-END mice. Up-regulation, yellow; down-regulation, blue; no change, black. (**E-G**) qPCR validation of PGC-1α and its downstream targets in (**E**) heart, (**F**) HSC, and (**G**) SC of WT, PolG-SED, and PolG-END (n = 6-8/group). Asterisk (PolG-SED *vs.* both WT and PolG-END): * $P < 0.05$. Error bars represent SEM. AU, *arbitrary units*.

Figure S3

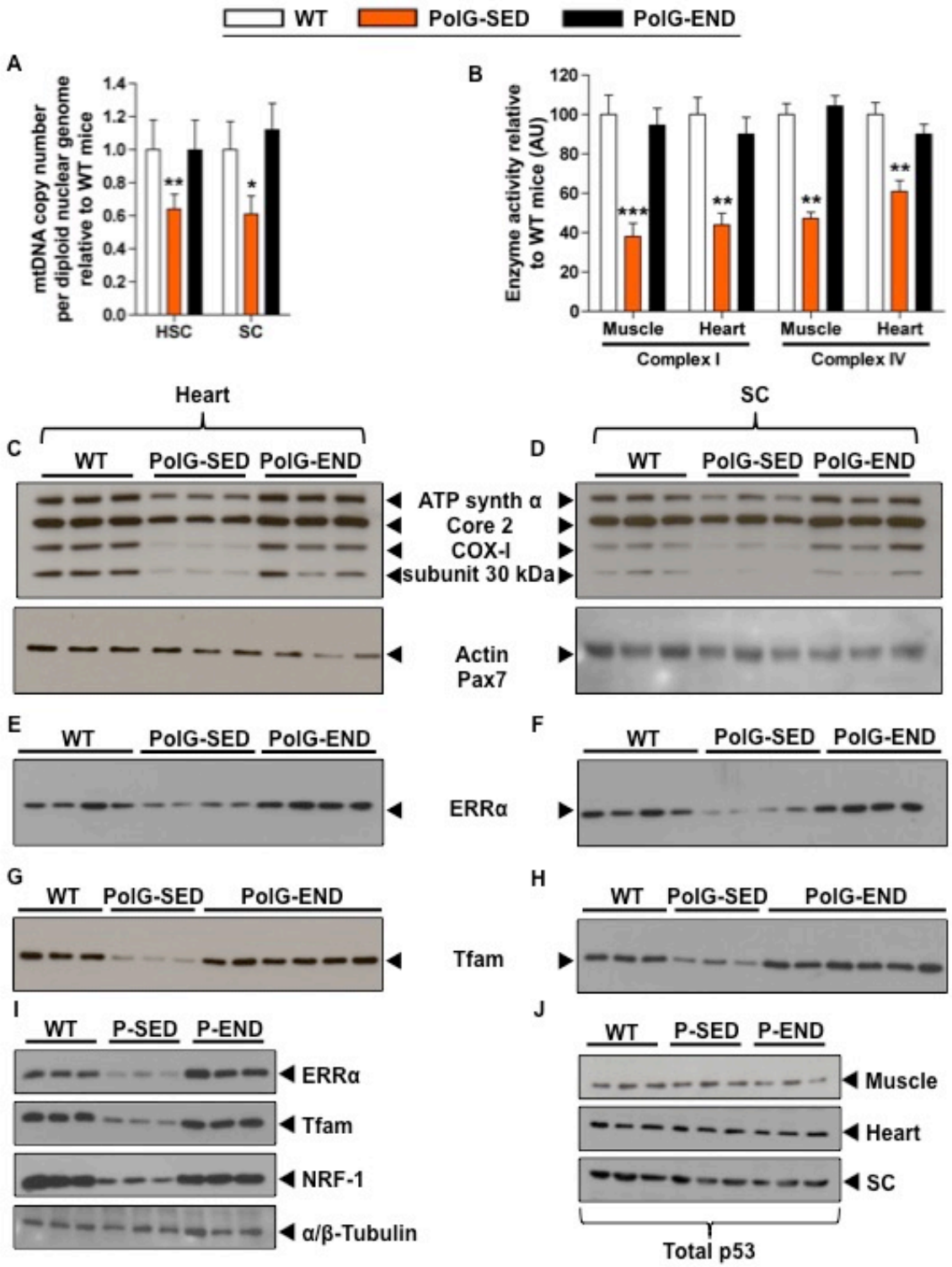
WT
PolG-SED
PolG-END
A
mtDNA copy number per diploid nuclear genome relative to WT mice
HSC
SC
B
Enzyme activity relative to WT mice (AU)
Muscle
Heart
Muscle
Heart
Complex I
Complex IV
Heart
SC
C
D
ATP synth α
Core 2
COX-I
subunit 30 kDa
Actin
Pax7
E
F
ERRα
G
H
Tfam
I
J
P-SED
P-END
ERRα
Tfam
NRF-1
α/β-Tubulin
Muscle
Heart
SC
Total p53

Figure S3. Endurance exercise promotes systemic mitochondrial biogenesis in mtDNA mutator mice. (**A**) mtDNA copy number of HSC and SC from WT, PolG-SED, and PolG-END mice (n = 4-5/group). (**B**) Mitochondrial complex I and complex IV activity in muscle and heart of WT, PolG-SED, and PolG-END mice (n = 4-5/group). (**C-H**) Representative blots of mitochondrial OXPHOS subunits (top to bottom: CV-ATP5 alpha subunit (~55 kDa), CIII-UQCRC2 subunit (~48 kDa), CIV subunit I (~40 kDa), and CII-SDHB (~30kDa)), estrogen-related receptor alpha (ERRα; ~50 kDa) and mitochondrial transcription factor A (Tfam; ~ 24 kDa) in heart (**C**, **E**, **G**) and SC (**D**, **F**, **H**) whole homogenate of WT, PolG-SED, and PolG-END (n = 4-6/group). (**I**) Representative blots of ERRα (~50 kDa), Tfam (~24 kDa), and nuclear-respiratory factor 1 (NRF-1; ~68 kDa) in muscle whole homogenate of WT, PolG-SED, and PolG-SED (n = 4-6/group). (**J**) Representative blots of total p53 (~53 kDa) in muscle, heart, and SC homogenates of WT, PolG-SED, and PolG-END (n = 5/group). Asterisk (PolG-SED vs. both WT and PolG-END): * $P < 0.05$, ** $P < 0.01$, *** $P < 0.001$. Error bars represent SEM. AU, *arbitrary units*.

Figure S4.

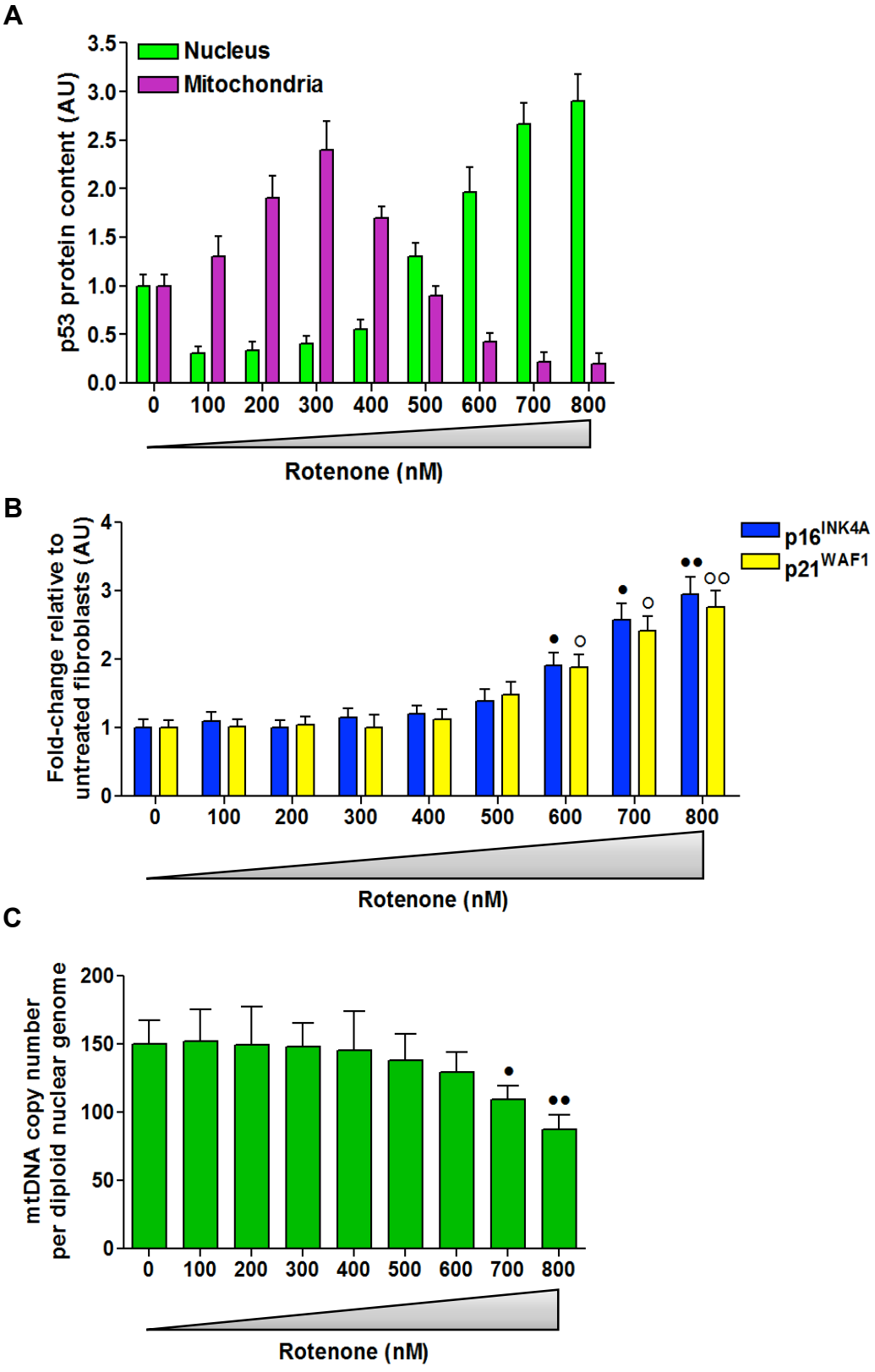
A
Nucleus
Mitochondria
p53 protein content (AU)
0.0
0.5
1.0
1.5
2.0
2.5
3.0
3.5
0
100
200
300
400
500
600
700
800
Rotenone (nM)
B
p16INK4A
p21WAF1
Fold-change relative to untreated fibroblasts (AU)
0
1
2
3
4
Rotenone (nM)
C
mtDNA copy number per diploid nuclear genome
0
50
100
150
200
Rotenone (nM)

2

Figure S4. Magnitude of mitochondrial ROS (physiological *vs.* pathological) regulates p53 subcellular localization. (**A**) Mouse fibroblasts were treated with increasing concentrations of rotenone (mitochondrial complex I inhibitor known to increase mitochondrial ROS in a dose-dependent fashion) to assess the nuclear vs. mitochondrial p53 content (n = 3). (**B**) mRNA expression of $p16^{INK4a}$ and $p21^{WAF1}$ (downstream targets of nuclear p53) and (**C**) mtDNA copy number in mouse fibroblasts treated with increasing concentrations of rotenone (n = 3). ● $P < 0.05$, ●● $P < 0.01$; ○ $P < 0.05$, ○○ $P < 0.05$. Error bars represent SEM. AU, *arbitrary units*.

Figure S5.

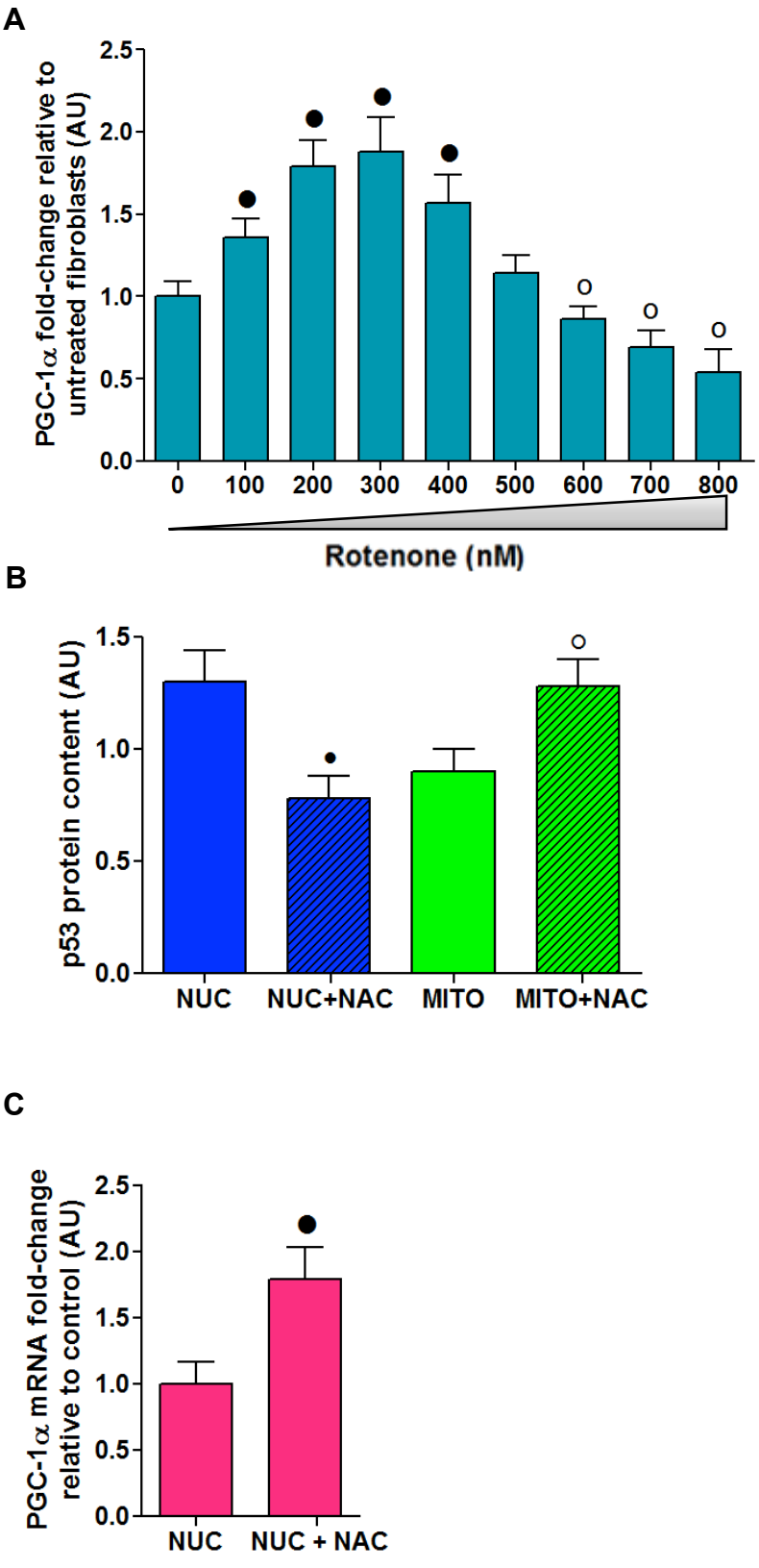
A
PGC-1α fold-change relative to untreated fibroblasts (AU)
2.5
2.0
1.5
1.0
0.5
0.0
0
100
200
300
400
500
600
700
800
Rotenone (nM)
B
p53 protein content (AU)
1.5
1.0
0.5
0.0
NUC
NUC+NAC
MITO
MITO+NAC
C
PGC-1α mRNA fold-change relative to control (AU)
2.5
2.0
1.5
1.0
0.5
0.0
NUC
NUC + NAC

2

Figure S5. Pre-treatment with exogenous antioxidant preferentially shuttles p53 to mitochondria in response to stress. (**A**) PGC-1α mRNA expression in mouse fibroblasts treated with increasing concentrations of rotenone (n = 3). ● greater than 0 nM rotenone $P < 0.05$; ○ lower than 0 nM rotenone $P < 0.05$. (**B-C**) Fibroblasts were pre-incubated for one hour with 3 mM *N*-acetyl-L-cysteine (NAC; ROS scavenger) followed by 500 nM rotenone treatment to assess (**B**) nuclear *vs.* mitochondrial content of p53 and (**C**) PGC-1α mRNA expression. NUC vs. NUC+NAC: ● $P < 0.05$; MITO vs. MITO+NAC: ○ $P < 0.05$. Error bars represent SEM. AU, *arbitrary units*.

Figure S6.

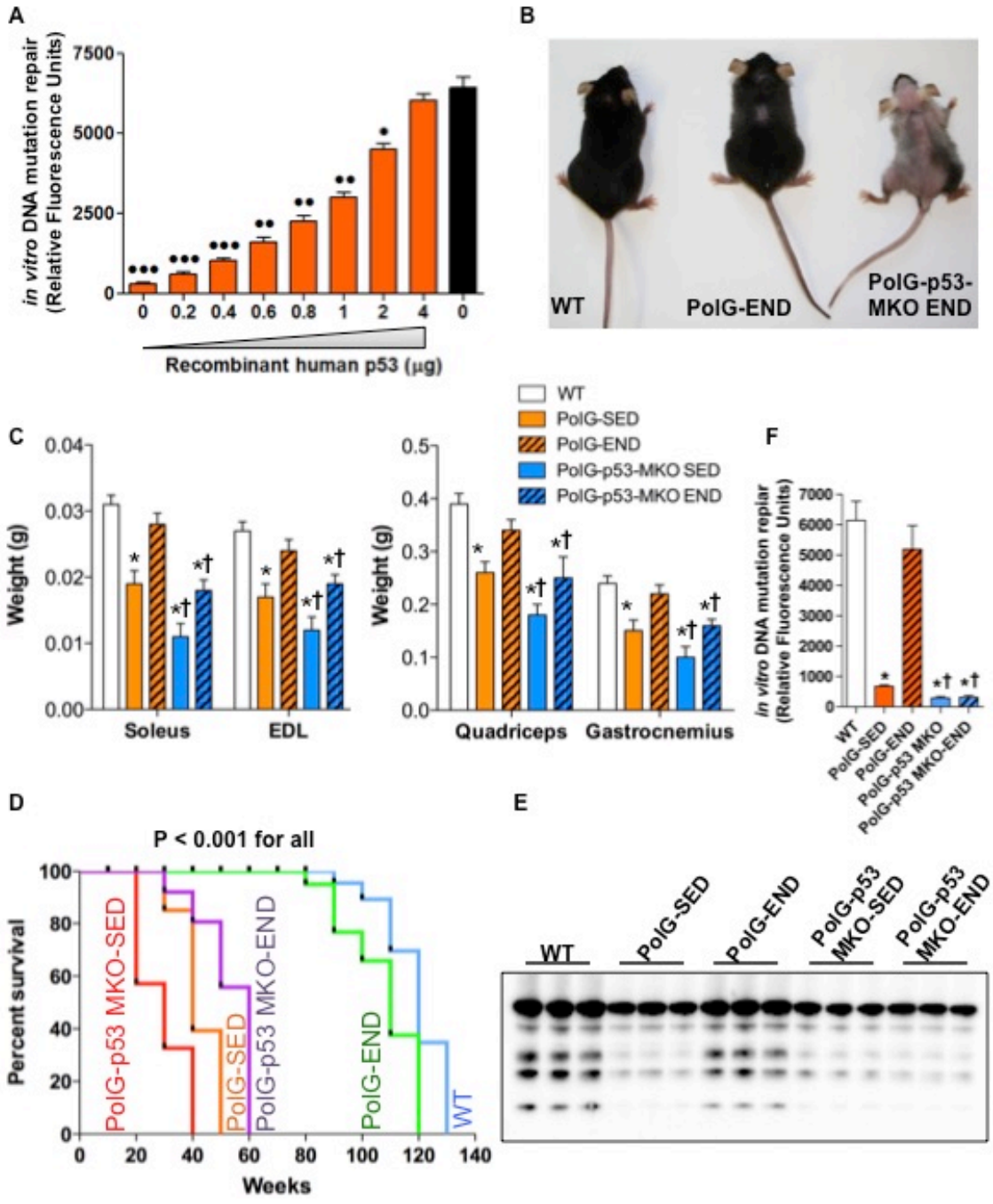
A
in vitro DNA mutation repair (Relative Fluorescence Units)
7500
5000
2500
0
0 0.2 0.4 0.6 0.8 1 2 4 0
Recombinant human p53 (µg)
B
WT
PolG-END
PolG-p53-MKO END
C
WT
PolG-SED
PolG-END
PolG-p53-MKO SED
PolG-p53-MKO END
Weight (g)
Soleus
EDL
Quadriceps
Gastrocnemius
F
in vitro DNA mutation repiar (Relative Fluorescence Units)
WT
PolG-SED
PolG-END
PolG-p53 MKO
PolG-p53 MKO-END
D
P < 0.001 for all
Percent survival
PolG-p53 MKO-SED
PolG-SED
PolG-p53 MKO-END
PolG-END
WT
Weeks
E
WT
PolG-SED
PolG-END
PolG-p53 MKO-SED
PolG-p53 MKO-END

Figure S6. Endurance exercise-mediated attenuation of sarcopenia, increase in endurance capacity, skeletal muscle mitochondrial biogenesis, and repair of muscle mtDNA mutations is p53 dependent. (**A**) Recombinant human p53 enhances mutation repair in muscle mitochondrial extracts from PolG-SED (n = 5/group). (**B**) Representative images of WT, PolG-SED, and PolG-p53 MKO-END mice are displayed. The PolG-p53 MKO-END mice shows no rescue progressive reduction in body size, increased kyphosis, loss of hair pigmentation and alopecia in comparison with littermate wild-type (WT) mice. Endurance exercise dramatically reversed the visible features of premature aging in PolG mice (PolG-END). (**C**) Weight of skeletal muscle: soleus, extensor digitorum longus (EDL), quadriceps femoris, and gastrocnemius in WT, PolG-SED, PolG-END, PolG-p53 MKO-SED, and PolG-p53 MKO-END mice (n = 5-8/group). (**D**) Kaplan-Meier survival probability. The logrank test was used to test for significant differences in life span distribution between groups. (**E**) Representative Western blot of muscle mitochondrial OXPHOS subunits (top to bottom: CV-ATP5 alpha subunit (~55 kDa), CIII-UQCRC2 subunit (~48 kDa), CIV subunit I (~40 kDa), CII-SDHB (~30kDa), and CI- NDUFB8 subunit (~20 kDa)) in WT, PolG-SED, PolG-END, PolG-p53 MKO-SED, and PolG-p53 MKO-END mice (n = 4-6/group). (**F**) A fluorescence-based in vitro DNA primer extension-mutation repair assay in muscle mitochondrial extracts from WT, PolG-SED, PolG-END, PolG-p53 MKO-SED, and PolG-p53 MKO-END mice (n = 4-5/group) to assess the excision of the unpaired artificial point mutations. Asterisk (PolG-SED *vs.* both WT and PolG-END): * $P < 0.05$; dagger (PolG-p53 MKO-SED *vs.* PolG-SED

OR PolG-p53 MKO-END vs. PolG-END): † $P < 0.05$; closed circle (PolG-END vs. PolG-SED): ● $P < 0.05$, ●● $P < 0.01$, ●●● $P < 0.001$. Error bars represent SEM. AU, *arbitrary units*.

Table S1: WT, PolG-SED, and PolG-END Skeletal Muscle Microarray IPA-GO Analysis

GO Categories	SEQ_ID	Gene_Name	Description	PolG-SED/WT Fold change	PolG-END/PolG-SED Fold change
Oxidative Phosphorylation	NM_007506	Atp5g1	ATP synthase, H+ transporting, mitochondrial F0 complex, subunit c (subunit 9), isoform 1	0.789	1.117
Oxidative Phosphorylation	NM_199008	Cox11	COX11 homolog, cytochrome c oxidase assembly protein (yeast)	0.708	1.128
Oxidative Phosphorylation	BC059729	Ndufa11	NADH dehydrogenase (ubiquinone) 1 alpha subcomplex 11	0.881	1.262
Oxidative Phosphorylation	NM_028177	Ndufab1	NADH dehydrogenase (ubiquinone) 1, alpha/beta subcomplex, 1	0.786	1.416
Oxidative Phosphorylation	AK011124	Ndufs4	NADH dehydrogenase (ubiquinone) Fe-S protein 4	0.783	1.284
Oxidative Phosphorylation	BC021616	Ndufs8	NADH dehydrogenase (ubiquinone) Fe-S protein 8	0.740	1.295
Oxidative Phosphorylation	XM_001004994	Ndufv2	NADH dehydrogenase (ubiquinone) flavoprotein 2	0.899	1.213
Oxidative Phosphorylation	NM_026438	Ppa1	pyrophosphatase (inorganic) 1	0.785	1.144
Oxidative Phosphorylation	NM_028009	Rpusd1	RNA pseudouridylate synthase domain containing 1	0.783	1.264
Oxidative Phosphorylation	BC013509	Sdhb	succinate dehydrogenase complex, subunit B, iron sulfur (Ip)	0.865	1.184
Oxidative Phosphorylation	BC034408	Uqcr	ubiquinol-cytochrome c reductase (6.4kD) subunit	0.937	1.131
Oxidative Phosphorylation	NM_025899	Uqcrc2	ubiquinol cytochrome c reductase core protein 2	0.831	1.062
Oxidative Phosphorylation	NM_025710	Uqcrfs1	1	0.829	1.065
GO Categories	**SEQ_ID**	**Gene_Name**	**Description**	**PolG-SED/WT Fold change**	**PolG-SED/PolG-END Fold change**
Mitochondrial Function	NM_199008	Cox11	COX11 homolog, cytochrome c oxidase assembly protein (yeast)	0.708	1.128
Mitochondrial Function	NM_173740	Maoa	monoamine oxidase A	1.296	0.686
Mitochondrial Function	BC059729	Ndufa11	NADH dehydrogenase (ubiquinone) 1 alpha subcomplex 11	0.881	1.262
Mitochondrial Function	NM_028177	Ndufab1	NADH dehydrogenase (ubiquinone) 1, alpha/beta subcomplex, 1	0.786	1.416
Mitochondrial Function	NM_027175	Ndufaf1	NADH dehydrogenase (ubiquinone) 1 alpha subcomplex, assembly factor 1	0.756	1.091
Mitochondrial Function	AK011124	Ndufs4	NADH dehydrogenase (ubiquinone) Fe-S protein 4	0.783	1.284
Mitochondrial Function	BC021616	Ndufs8	NADH dehydrogenase (ubiquinone) Fe-S protein 8	0.740	1.295
Mitochondrial Function	XM_001004994	Ndufv2	NADH dehydrogenase (ubiquinone) flavoprotein 2	0.899	1.213
Mitochondrial Function	BC013509	Sdhb	succinate dehydrogenase complex, subunit B, iron sulfur (Ip)	0.865	1.184
Mitochondrial Function	NM_025899	Uqcrc2	ubiquinol cytochrome c reductase core protein 2	0.831	1.062
Mitochondrial Function	NM_025710	Uqcrfs1	1	0.829	1.065

GO Categories	SEQ_ID	Gene_Name	Description	PolG-SED/WT Fold change	PolG-SED/PolG-END Fold change
Glycolysis/Gluconeogenesis	NM_019811	Acss2	acyl-CoA synthetase short-chain family member 2	0.714	1.252
Glycolysis/Gluconeogenesis	BC100730	Adh4	alcohol dehydrogenase 4 (class II), pi polypeptide	0.824	1.230
Glycolysis/Gluconeogenesis	NM_027406	Aldh1l1	aldehyde dehydrogenase 1 family, member L1	0.636	1.127
Glycolysis/Gluconeogenesis	NM_175438	Aldh4a1	aldehyde dehydrogenase 4 family, member A1	0.642	1.222
Glycolysis/Gluconeogenesis	NM_138600	Aldh7a1	aldehyde dehydrogenase family 7, member A1	0.757	1.044
Glycolysis/Gluconeogenesis	BC026680	Dlat	dihydrolipoamide S-acetyltransferase (E2 component of pyruvate dehydrogenase complex)	0.803	1.234
Glycolysis/Gluconeogenesis	NM_010292	Gck	glucokinase	0.663	1.179
Glycolysis/Gluconeogenesis	NM_013820	Hk2	hexokinase 2	0.781	1.189
Glycolysis/Gluconeogenesis	AK076803	Pfkp	phosphofructokinase, platelet	1.110	1.064
GO Categories	**SEQ_ID**	**Gene_Name**	**Description**	**PolG-SED/WT Fold change**	**PolG-SED/PolG-END Fold change**
Oxidative Stress	BC062138	Actc1	actin, alpha, cardiac	1.999	0.605
Oxidative Stress	BC021796	Actg1	actin, gamma, cytoplasmic 1	1.310	0.974
Oxidative Stress	BC057876	Dnaja1	DnaJ (Hsp40) homolog, subfamily A, member 1	0.803	1.145
Oxidative Stress	BC022948	Dnaja4	DnaJ (Hsp40) homolog, subfamily A, member 4	0.761	1.609
Oxidative Stress	NM_010357	Gsta4	glutathione S-transferase, alpha 4	0.817	1.172
Oxidative Stress	BC058163	Gstk1	glutathione S-transferase kappa 1	0.707	1.305
Oxidative Stress	NM_008183	Gstm2	glutathione S-transferase, mu 2	0.820	0.954
Oxidative Stress	NM_010359	Gstm3	glutathione S-transferase, mu 3	0.996	0.949
Oxidative Stress	NM_010361	Gstt2	glutathione S-transferase, theta 2	1.140	0.962
Oxidative Stress	BC002081	Jun	Jun oncogene	0.676	1.353
Oxidative Stress	NM_001025577	Maf	avian musculoaponeurotic fibrosarcoma (v-maf) AS42 oncogene homolog	1.201	0.937
Oxidative Stress	NM_016737	Stip1	stress-induced phosphoprotein 1	0.795	1.203

GO Categories	SEQ_ID	Gene_Name	Description	PolG-SED/WT Fold change	PolG-SED/PolG-END Fold change
Free Radical Scavenging	BC049768	Alox5	arachidonate 5-lipoxygenase	0.907	1.069
Free Radical Scavenging	BC095964	Bcl2	B-cell leukemia/lymphoma 2	0.863	1.344
Free Radical Scavenging	BC064058	Cd28	CD28 antigen	1.138	0.758
Free Radical Scavenging	NM_013706	Cd52	CD52 antigen	1.309	0.808
Free Radical Scavenging	NM_007779	Csf1r	colony stimulating factor 1 receptor	1.121	1.003
Free Radical Scavenging	NM_001012477	Cxcl12	chemokine (C-X-C motif) ligand 12	1.454	0.973
Free Radical Scavenging	NM_007807	Cybb	cytochrome b-245, beta polypeptide	1.633	0.643
Free Radical Scavenging	NM_007837	Ddit3	DNA-damage inducible transcript 3	0.749	1.261
Free Radical Scavenging	BC017681	Egf	epidermal growth factor	1.264	0.727
Free Radical Scavenging	NM_007953	Esrra	estrogen related receptor, alpha	0.760	1.288
Free Radical Scavenging	M13226	Gzma	granzyme A	0.816	1.184
Free Radical Scavenging	NM_013820	Hk2	hexokinase 2	0.781	1.189
Free Radical Scavenging	NM_001012401	Hspb6	heat shock protein, alpha-crystallin-related, B6	0.852	1.317
Free Radical Scavenging	NM_010493	Icam1	intercellular adhesion molecule	1.468	0.785
Free Radical Scavenging	AK033126	Immt	inner membrane protein, mitochondrial	0.830	1.160
Free Radical Scavenging	NM_010577	Itga5	integrin alpha 5 (fibronectin receptor alpha)	0.810	1.257
Free Radical Scavenging	BC002081	Jun	Jun oncogene	0.676	1.353
Free Radical Scavenging	BC094612	Ltbp1	latent transforming growth factor beta binding protein 1	1.212	0.898
Free Radical Scavenging	NM_027175	Ndufaf1	NADH dehydrogenase (ubiquinone) 1 alpha subcomplex, assembly factor 1	0.756	1.091
Free Radical Scavenging	BC006703	Prnp	prion protein	0.799	1.157
Free Radical Scavenging	AK085938	Prodh	proline dehydrogenase	0.882	1.282
Free Radical Scavenging	AK141959	Ralgds	ral guanine nucleotide dissociation stimulator	1.358	0.922
Free Radical Scavenging	BC055340	Slc2a1	solute carrier family 2 (facilitated glucose transporter), member 1	0.593	1.540
Free Radical Scavenging	NM_011421	Smpd1	sphingomyelin phosphodiesterase 1, acid lysosomal	0.818	1.215
Free Radical Scavenging	NM_025710	Uqcrfs1	ubiquinol-cytochrome c reductase, Rieske iron-sulfur polypeptide 1	0.829	1.065
Free Radical Scavenging	NM_011693	Vcam1	vascular cell adhesion molecule 1	1.287	0.791

GO Categories	SEQ_ID	Gene_Name	Description	PolG-SED/WT Fold change	PolG-SED/PolG-END Fold change
DNA Damage Repair	NM_175086	Agtr1b	angiotensin II receptor, type 1b	0.949	1.178
DNA Damage Repair	BC049768	Alox5	arachidonate 5-lipoxygenase	0.907	1.069
DNA Damage Repair	BC095964	Bcl2	B-cell leukemia/lymphoma 2	0.863	1.344
DNA Damage Repair	BC044841	Ccnd1	cyclin D1	1.409	0.830
DNA Damage Repair	NM_007642	Cd28	CD28 antigen	1.838	0.505
DNA Damage Repair	NM_007651	Cd53	CD53 antigen	1.592	0.721
DNA Damage Repair	NM_001012477	Cxcl12	chemokine (C-X-C motif) ligand 12	1.454	0.973
DNA Damage Repair	NM_007837	Ddit3	DNA-damage inducible transcript 3	0.749	1.261
DNA Damage Repair	BC017681	Egf	epidermal growth factor	1.264	0.727
DNA Damage Repair	NM_007953	Esrra	estrogen related receptor, alpha	0.760	1.288
DNA Damage Repair	NM_133765	Fbxo31	F-box only protein 31	0.726	1.071
DNA Damage Repair	NM_008046	Fst	follistatin	1.409	0.762
DNA Damage Repair	NM_020567	Gmnn	geminin	0.608	1.436
DNA Damage Repair	NM_010370	Gzma	granzyme A	0.978	1.014
DNA Damage Repair	NM_010567	Inppl1	inositol polyphosphate phosphatase-like 1	0.785	1.223
DNA Damage Repair	NM_010591	Jun	Jun oncogene	0.797	1.265
DNA Damage Repair	NM_013823	Kl	klotho	1.259	0.851
DNA Damage Repair	L04275	Msr1	macrophage scavenger receptor 1	1.058	1.038
DNA Damage Repair	NM_011853	Oas1b	2'-5' oligoadenylate synthetase 1B	1.391	0.674
DNA Damage Repair	NM_133752	Opa1	optic atrophy 1 homolog (human)	0.887	1.129
DNA Damage Repair	AK032149	Ppargc1a	peroxisome proliferative activated receptor, gamma, coactivator 1 alpha	0.798	1.585
DNA Damage Repair	NM_011170	Prnp	prion protein	0.754	1.190
DNA Damage Repair	NM_148945	Rps6ka3	ribosomal protein S6 kinase polypeptide 3	1.102	0.872
DNA Damage Repair	NM_009477	Upp1	uridine phosphorylase 1	1.044	1.029
GO Categories	**SEQ_ID**	**Gene_Name**	**Description**	**PolG-SED/WT Fold change**	**PolG-SED/PolG-END Fold change**
Fatty Acid Metabolism	BC060650	Aldh4a1	aldehyde dehydrogenase 4 family, member A1	0.623	1.166
Fatty Acid Metabolism	BC045199	Acad11	acyl-Coenzyme A dehydrogenase family, member 11	0.767	1.157
Fatty Acid Metabolism	NM_007383	Acads	acyl-Coenzyme A dehydrogenase, short chain	0.682	1.315
Fatty Acid Metabolism	NM_025826	Acadsb	acyl-Coenzyme A dehydrogenase, short/branched chain	0.732	1.185
Fatty Acid Metabolism	BC100730	Adh4	alcohol dehydrogenase 4 (class II), pi polypeptide	0.824	1.230

Table S2. Real-time PCR primer sequences.

Gene	Forward primer (5' → 3')	Reverse primer (5' → 3')
PGC-1α	ttccaccaagagcaagtat	cgctgtcccatgaggtatt
Tfam	gaagggaatgggaaaggtaga	aacaggacatggaaagcagat
ALAS	aagggcactggtcggttta	ctgagggactcgggataaga
COX-I	ctagccgcaggcattactat	tgcccaaagaatcagaacag
COX-IV	ctccaacgaatggaagacag	tgacaaccttcttagggaac
ND1	gtggctcatctactccactga	tcgagcgatccataacaataa
ATPase 6	gacgaacatgaaccctaat	tacggctccagctcatagt
ERRα	cctcttgaagaaggctttgca	gcagggcagtgggaagcta
NRF-1	gaactgccaaccacagtcac	tttgttccacctctccatca
$p21^{WAF1}$	ggagcaaagtgtgccgttgtc	gaggaagtactgggcctcttg
$p16^{INK4a}$	cccaacgccccgaact	aacgttgcccatcatcatca
Telomere	cggtttgtttgggtttgggtttgggtttgggtttgggtt	ggcccttaccctta ccccttaccctta ccctta ccct
36B4	actggtctaggacccgagaag	tcaatggtgcctctggagatt
β-2 microglobulin	ggtctttctggtgcttgtct	tatgttcggcttcccattct
mtDNA cytochrome *b*	catttattatcgcggcccta	tgttgggttgtttgatcctg
mtDNA COX-II	gccgactaaatcaagcaaca	caatgggcataaagctatgg
β-globin	gaagcgattctagggagcag	ggagcagcgattctgagtaga
PGC-1α promoter (-564 position)	tcatggatgtgctgggttag	cagatggttgcttgcactaga
PGC-1α promoter (-954 position)	ccacgaaagaatcatgagg	aaccgccacatttgtttagg
mtDNA template (*mismatch mutation*)	cagatactgcgacatag*cca*	gtctatgacgctgtatcccacgaggccga ggtcgcagagc